

Temperature gradient in Hall thrusters

D. Staack,^{a)} Y. Raitsev, and N. J. Fisch

Princeton Plasma Physics Laboratory, Princeton University, Princeton, New Jersey 08540

(Received 16 October 2003; accepted 24 February 2004)

Plasma potentials and electron temperatures were deduced from emissive and cold floating probe measurements in a 2 kW Hall thruster, operated in the discharge voltage range of 200–400 V. An almost linear dependence of the electron temperature on the plasma potential was observed in the acceleration region of the thruster both inside and outside the thruster. This result calls into question whether secondary electron emission from the ceramic channel walls plays a significant role in electron energy balance. The proportionality factor between the axial electron temperature gradient and the electric field is also significantly smaller than might be expected by fluid models. © 2004 American Institute of Physics. [DOI: 10.1063/1.1710732]

A conventional magnetic layer Hall thruster is a crossed field electric discharge device with a radial magnetic field and axial electric field applied in a coaxial channel.¹ The ions are electrostatically accelerated through the azimuthally rotating cloud of magnetized electrons. Secondary electron emission (SEE) from the ceramic channel walls is considered to be a major effect limiting the electron temperature in the thruster. Current analytical models^{2,3} rely on SEE effects to produce operational characteristics similar to experiments. The use of such theoretical models has not, however, been justified in detail.

In recent experiments, emissive and cold probe floating potential profiles were used to estimate the plasma potential and electron temperature in the PPPL 2 kW laboratory Hall thruster for discharge voltages in a range of 200–400 V. These measurements indicate no limitation by SEE of the walls on the electron temperature below 40 eV, which tends not to support existing theoretical models. They also exhibit a yet unexplained mechanism of electron energy loss proportional to the electric field.

The 2 kW PPPL laboratory Hall thruster and test facility have been described in detail elsewhere.⁴ The vacuum facility is a 28 m³ vessel with two CVI cryogenic pumps providing $\sim 10^{-5}$ Torr background pressure when operating the thruster. The thruster has inner and outer diameters of 73 and 123 mm, respectively. The channel was made entirely of boron nitride HP grade.

The electron temperature and plasma potential measurements were made using emissive and cold probes⁵ which were rapidly inserted and removed from the thruster while the floating potential of the filament tip was measured. These potentials are related to the electron temperature and plasma potential.⁶ For xenon we have $T_e = (\phi_e - \phi_c)/4.27$ and $\phi = \phi_e + 1.5T_e$ where T_e is the electron temperature, ϕ is the plasma potential, and ϕ_c and ϕ_e are the cold and emissive probe floating potentials. Although the electron energy distribution may depart from an isotropic Maxwellian, which was used in derivation of these equations, the results presented below still reflect an averaged electron energy, and hence qualitatively reflect the actual physical processes. The

probe design and thruster operating regimes were chosen to minimize probe-induced perturbations.⁷ The results are only shown for regions where the probe induced changes in thruster discharge current were less than 15%, and the changes in the floating potential of a fixed Langmuir probe mounted 2 mm inside the thruster exit plane were less than 25 V.

Figure 1 shows the electron temperature and plasma potential profiles calculated from the emissive and floating probe potential profiles when the thruster was operated at a discharge voltage of 300 V and an anode gas flow rate of 5.0 mg/s. Outside the thruster the temperature is greater than 14 eV beginning about 20 mm from the exit plane. The temperature peaks at a value of about 37 eV, 4 mm inside the thruster. For this measurement the change in discharge current during probe insertion was less than 5% and the changes in stationary probe voltage were less than 8 V. The standard deviations of the averaged probe measurements were at most 12 V. Based upon the perturbations and the standard deviations for this measurement the error in plasma potential is less than 20 V and the error in electron temperature is less than 4 eV.

Figure 2 is a plot of the electron temperature as a function of the plasma potential. This T_e - ϕ plot is a very useful indication of the electron energy gain. Three distinct regions are noted a cathode/plume region, the acceleration region, and the ionization region. The electron temperature varies nearly linearly with the plasma potential in the acceleration

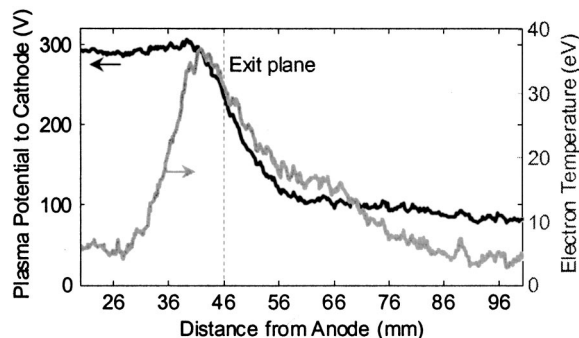


FIG. 1. Plasma potential and electron temperature profiles for 300 V discharge voltage, 5.0 mg/s xenon flow rate, and 4.56 A discharge current.

^{a)}Electronic mail: dstaack@princeton.edu

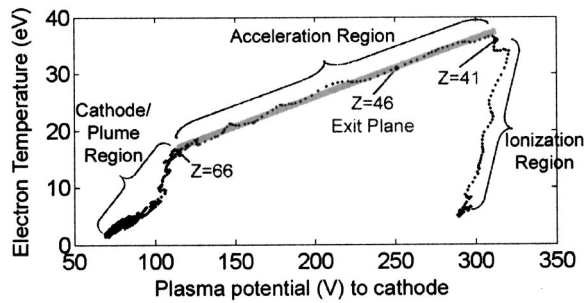


FIG. 2. Electron temperature vs plasma potential for 300 V discharge voltage, 5.0 mg/s xenon flow rate, and 4.56 A discharge current; Z indicates the distance from the anode.

region. A linear fit to this region is accurate within ± 2 eV and yields the equation: $T_e = 0.10\phi + 5.2$. This linearity is also visible between the independently measured cold and emissive floating potentials.

The linear dependence of the electron temperature on the plasma potential can be simply put as an energy relationship in the form $dT_e/dz = -\beta E$ with $\beta = 0.10$, where the electric field $E = -d\phi/dz$. A simplified electron energy equation of the form $T_e = \beta\phi$ has been suggested in the past for Hall thrusters.⁸ We derived an equation of this form with a value of $\beta = 0.4$ beginning with an energy equation similar to Eq. (7) in Ref. 2, and then considering only electron heating in the electric field, neglecting energy transfer to other species and neglecting thermal conduction. Such an equation assumes all the potential energy of the electron is converted into internal energy and pressure. As can be seen from Fig. 3 the measured value of β is significantly smaller and in the range of 0.08–0.14. For the cases shown the linear relationship holds both inside and outside the thruster for electron temperatures up to 40 eV.

Theoretical models of Hall thrusters generally use a Maxwellian or bi-Maxwellian electron distribution function. The presence of high SEE from ceramic channel walls then limits the electron temperature in the plasma. This electron

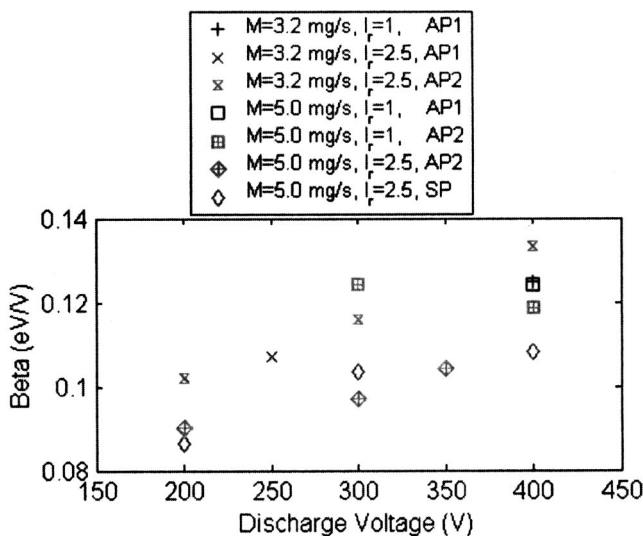


FIG. 3. Linear fit parameter β for several discharge voltages, mass flow rates (M), inner to outer magnetic coils current ratios (I_r), and probe design (AP=unshielded alumina probe holder, SP=segmented graphite shielded probe holder) (see Ref. 7).

cooling mechanism is most effective for SEE of about 100% when the sheath becomes space charge limited.⁹ For boron nitride ceramic walls and a Maxwellian electron distribution, the critical electron temperature is about 17 eV.¹⁰ The precise temperature depends on the experimental data used for SEE properties of the material. Contrary to these theoretical predictions, our measurements show that the linear relationship holds both inside and outside the thruster channel for electron temperatures up to 40 eV. A Maxwellian distribution function with a truncated high-energy tail has been shown by Ref. 11 to have a lower effective SEE and so a higher critical temperature; however, their estimates were only for electron temperatures around 20 eV. Similar estimates using non-Maxwellian distribution functions with average electron energy of around 40 eV show the effective SEE can be less than 100%.

$T_e - \phi$ diagrams, for comparison, were deduced from published data. High spatial resolution experimental data on different hall thrusters^{12–14} is available and Refs. 12 and 13 show the same linear trend in the $T_e - \phi$ diagram over the acceleration region, and ionization region, though the cathode/plume region is not as distinct. Reference 13 uses a similar method to determine the electron temperature, and shows a definite linear relationship at 100, 160, and 200 V in the acceleration region both inside and outside the thruster with $\beta = 0.09, 0.13,$ and $0.14,$ respectively. Reference 12, which is the 90 mm outer diameter PPPL Hall thruster, has a β of 0.15 for 250 V operation. The $T_e - \phi$ diagram of Ref. 14, which uses double probe characteristics to determine the electron temperature, has a different structure and no linear region is observable.

$T_e - \phi$ diagrams from analytical models^{2,3} do not show a linear relationship over the entire acceleration region. A region outside the thruster is approximately linear with a β of about 0.4, the same as derived for simple electron energy conversion. These model results nearly match the assumptions of the electron heating derivation because in this region collisions are negligible, the electron flux is nearly constant and thermal conductivity is not significant. The $T_e - \phi$ diagram of a fully kinetic 2D PIC code^{15,16} shows a linear relationship similar to that observed experimentally. For 300 and 400 V simulations the linear fit slopes are 0.1 and 0.13, in the range of those measured experimentally. The agreement between the kinetic code and the experiments indicates that there is an energy loss mechanism that is included in the kinetic model but is not included in the analytical models. However, in the PIC code the linear relationship ends at the thruster exit plane where the temperature is a maximum. This indicates that in the PIC model as in Refs. 2, 3, and 10 energy losses to the wall are more significant than deduced from experiment. Another kinetic code¹⁷ does not show the same linear relationship and also has much lower electron temperatures than measured experimentally for similar discharge voltages.

Some insight into the nature of the electron energy loss mechanism can be gained by considering the electron energy balance for the conditions shown in Figs. 1 and 2. In the acceleration region the electrons gain about 200 eV in potential energy and about 20 eV in temperature. 5/2 times the change in temperature corresponds to the energy stored in-

ternally in the internal and mechanical (pressure) energy. From the measurements about 50 eV or 25% of the potential energy gained is converted to internal energy. Using the measured electric field and magnetic field the maximum azimuthal drift energy is 6 eV or, at most including the axial drift energy, about 4% of the potential energy gained. The remaining about 70% of the potential energy gained needs to be convected or conducted out of the acceleration region or lost. Loss processes relating to the walls or expansion are unlikely, since the measured proportionality between the temperature gradient and electric field is the same inside and outside the thruster and such processes should change at the thruster exit plane. Estimates of electron-neutral and electron-ion energy transfer rates show them to be negligible in the acceleration region. Furthermore, these terms along with convection and conduction are accounted for in the model of Ref. 2 and are insufficient to match experimental results. The only collision term of significance in the acceleration region is the anomalous collision frequency used by both kinetic and analytical models to enhance the axial electron transport to values measured experimentally. In most models this anomalous collision frequency is only used as a momentum loss term and does not affect the energy balance. The inclusion of an anomalous energy loss terms, radiative mechanism or possibly effects of non-Maxwellian distribution functions may need to be considered in order to accurately model the measured electron energy balance.

In conclusion, by plotting the electron temperature as a function of the plasma potential we found a linear dependence of the electron temperature gradient on the electric field for several Hall thrusters and for a variety of operating regimes. The constant of proportionality, β , ranges between 0.08 and 0.14 depending on the thruster and operating conditions. The value of β is significantly smaller than can be expected from fluid models and this indicates a yet unexplained energy loss term nearly proportional to the electric field. Furthermore, the linear relationship holds both inside and outside the thruster for electron temperature up to 40 eV,

indicating that the walls and SEE do not have a significant effect on the electron temperature over this operating range and for this wall material.

The authors would like to thank Artem Smirnov, and Leonid Dorf for their useful discussions and help with experiments. This work was supported by the NJ Commission on Science and Technology and the U.S. Department of Energy under Contract No. DE-AC0276-CHO3073.

- ¹A. Morosov and V. Savelyev, in *Review of Plasma Physics*, edited by B. Kadomtsev and V. Shafranov (Kluwer, Dordrecht, 2000), Vol. 21.
- ²E. Abedo, J. Gallardo, and M. Martinez-Sanchez, *Phys. Plasmas* **10**, 3397 (2003).
- ³M. Keidar and I. D. Boyd, *Phys. Plasmas* **8**, 5315 (2001), and additional model results from correspondence with author.
- ⁴Y. Raiteses, D. Staack, A. Dunaevsky, L. Dorf, and N. J. Fisch, *Proceeding of the 28th International Electric Propulsion Conference, March 2003, Toulouse, France* (Electric Rocket Propulsion Society, Cleveland, 2003), IEPC paper No. 03-0139.
- ⁵F. Chen, in *Plasma Diagnostic Techniques*, edited by R. Huddleston and S. Leonard (Academic, New York, 1965).
- ⁶Y. Raiteses, D. Staack, L. Dorf, and N. J. Fisch, *Proceedings of the 39th Joint Propulsion Conference and Exhibit, July 20–23, 2003, Huntsville, AL* (American Institute of Aeronautics and Astronautics, Reston, VA, 2003), AIAA paper No. 2003-5153.
- ⁷D. Staack, Y. Raiteses, and N. J. Fisch, *Rev. Sci. Instrum.* **75**, 393 (2004).
- ⁸A. V. Zharinov and Y. S. Popov, *Sov. Phys. Tech. Phys.* **12**, 208 (1967).
- ⁹G. D. Hobbs and J. A. Wesson, *Plasma Phys.* **9**, 85 (1967).
- ¹⁰E. Y. Choueiri, *Phys. Plasmas* **8**, 5025 (2001).
- ¹¹N. Meezan and M. Cappelli, *Phys. Rev. E* **66**, 036401 (2002).
- ¹²Y. Raiteses, M. Keidar, D. Staack, and N. J. Fisch, *J. Appl. Phys.* **92**, 4906 (2002).
- ¹³N. Meezan, W. Hargus, and M. Cappelli, *Phys. Rev. E* **63**, 026410 (2001).
- ¹⁴J. M. Haas and A. D. Gallimore, *Proceedings of the 36th Joint Propulsion Conference July 16–19, 2000, Huntsville, AL* (American Institute of Aeronautics and Astronautics, Reston, VA, 2000), AIAA paper No. 00-3422.
- ¹⁵J. Szabo, *Proceeding of the 27th International Electric Propulsion Conference, October 2001, Pasadena, CA* (Electric Rocket Propulsion Society, Cleveland, 2001), IEPC paper No. 01-341.
- ¹⁶N. Warner, J. Szabo, and M. Martinez-Sanchez, *Proceeding of the 28th International Electric Propulsion Conference, March 2003, Toulouse, France* (Electric Rocket Propulsion Society, Cleveland, 2003), IEPC paper No. 03-082.
- ¹⁷L. Garrigues, G. J. M. Hagelaar, J. Bareilles, C. Boniface, and J. P. Boeuf, *Phys. Plasmas* **10**, 4886 (2003).